Thermochimica Acta, 143 (1989) 27-35
Elsevier Science Publishers B.V., Amsterdam - Printed in The Netherlands

THEORY OF EMANATION THERMAL ANALYSIS. PART VIII. INFLUENCE OF SAMPLE-LABELLING CONDITIONS ON THE THERMOSTIMULATED INERT GAS RELEASE

A.V. SHELEZNOV and I.N. BECKMAN

Department of Radiochemistry and Chemical Technology, Moscow State University, 199 234 Moscow (U.S.S.R.)

V. BALEK

Nuclear Research Institute, 250 68 Rez (Czechoslovakia) (Received 2 June 1988)

ABSTRACT

The influence of the initial amount of inert gas in the solid sample on the temperature dependences of the thermostimulated gas release rate (TGR curves) was analysed. The methods of functional scales and of the analysis of temperature dependences of the effective diffusion activation energy were used. It is demonstrated that the shape of the TGR curves depends considerably on the conditions of the sample labelling, namely the inert gas pressure and the duration of the diffusion labelling of samples. The possibility of reconstructing the spectrum of the defect sites and their occupation by the inert gas is discussed.

INTRODUCTION

When the diffusion technique is used for the inert-gas labelling of solid samples, the gas is located at the defect sites at defined depths from the surface. The potential energies of different defect sites can be different. The amount of inert gas incorporated into the solid can be controlled by the partial pressure and the duration of inert-gas labelling as well as by the thermal pretreatment of the labelled samples and their outgassing.

It has been observed experimentally that the shape of the thermostimulated gas-release curves (TGR curves) depends on both the energy spectrum of the defect sites and the amount of the inert gas localized in the solid. In the preceding paper in this series [1] we used mathematical modelling to demonstrate the influence of the energy spectrum of the defect sites on the TGR curves. In the present study the influence of the amount of inert gas in the samples on the TGR curves was analysed. The influence of the occupation of the defect sites on the TGR curves is discussed on the basis of the results of the mathematical modelling. The methods of functional scales [2] and the analysis of the temperature dependences of the effective activation energy of gas diffusion were used.

The results obtained in this work can be used for the application of emanation thermal analysis in the investigation of porous solids and materials (such as silicagels, zeolites, etc.) labelled by the diffusion technique.

ENERGY SPECTRUM OF THE DEFECT SITES AND THEIR OCCUPATION BY THE INERT GAS

In the previous paper in this series [1], both the discrete and the continuous energy spectra of the defect sites were considered. The amount of gas localized at the defects of the *ith* type is given by the Langmuir law (in a dimensionless form)

$$\theta_i(E) = \frac{n_i}{n_{i,\infty}} = \frac{K_i(E)p}{1 + K_i(E)p} \tag{1}$$

where $n_{i,\infty}$ is the maximum capacity of the ith type defect of the inert gas, K_i is the equilibrium constant with respect to the defect site, and ρ is the partial pressure of the inert gas. The relationship $n_i = K_i p$ results from the Henry law.

However, it should be mentioned that, in practice, the TGR curves are measured under non-equilibrium conditions with a temperature increase at constant heating rates. The mechanism of the first-order reaction, the single-jump diffusion mechanism, is assumed.

We shall consider here a solid sample containing several defect sites characterized by the discrete-energy spectrum $N(E)$. When such a solid is maintained under a high inert-gas pressure, the defect sites will become occupied by the gas. Supposing that the defect sites are equally accessible for the inert gas, the inert gas will first be trapped on the sites of maximum energy. The distribution of the gas between the defect sites is given either by the Boltzman distribution function (in the case of partially occupated defect sites), or by the Fermi-Dirac distribution [3] (in the case of the complete occupation of the defect sites).

When the pressure of the inert gas is increased, the energy spectrum $N(E)$ of the inert gas located at the defects is similar to the energy spectrum $N(E)$ of the defect sites. Instead of the parameters $n(E)$ and $N(E)$ we shall use the dimensionless parameters

$$\theta^*(E) = \frac{n(E)}{N} \quad \text{and} \quad \phi(E) = \frac{N(E)}{N} \tag{2}$$

where N is the total number of defect sites in the solid sample. However, in practice it is more convenient to replace the parameter $\theta^*(E)$ with $\theta(E) = n(E)/n_\infty(E)$ where $n_\infty(E)$ is the maximum capacity characterized by the energy E.

The function $\varphi(E)$ is considered in the ETA experiments with thermo-stimulated release of the inert gas from the solids. When the function $\Phi\{E)$ is to be determined from the TGR measurements, the experiments must be performed under the conditions of complete occupation of the defect sites by the inert gas. Supposing that the inert gas adsorption at every site is controlled by the Langmuir equation, the amount of the inert gas located at the defect sites with energy E is given by eqn. (1).

The total amount, n, of the inert gas located in the solid sample is

$$n = \int_{E_{\min}}^{E_{\max}} n(E)\,\mathrm{d}E \tag{3}$$

where $E_{\min}$ and $E_{\max}$ are the limits of the energy spectrum $N(E)$ of the defect sites.

The mean concentration c of the inert gas in the solid is

$$\bar{c} = \frac{n}{V} \tag{4}$$

where V is the sample volume.

The typical dependence of θ on the pressure ρ is illustrated in Fig. 1 for different non-homogeneous solids

characterized by the discrete energy spectrum. From Fig. 1 (curve 1) it is obvious that at low-pressure values the dependence of θ on ρ is linear, whereas at higher values of the partial pressure θ is practically independent of p.

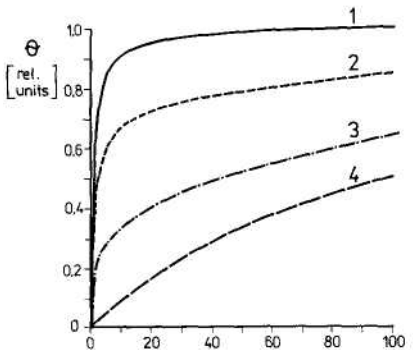

Fig. 1. Dependence of the inert-gas concentration in the solid sample on the partial pressure used in sample labelling (Langmuir adsorption isotherms). Curve 1: the gas adsorption on a homogeneous surface ($\theta_\infty = I$, $K = 1$). Curve 2: the gas adsorption on a heterogeneous surface characterized by two types of adsorption centres ($\theta_{1,\infty}$=l, K_1=1, $\phi_1 = 0.7$; and $\theta_{2,\infty} = 1$, $K_2 = 0.01$, $\phi_2 = 0.3$). Curve 3: the gas adsorption on a heterogeneous surface characterized by two types of adsorption centres ($\theta_{1,\infty}$=1, K_1=1, ϕ_1= 0.3; and $\theta_{2,\infty} = 1$, $K_2 = 0.01$, $\phi_2 = 0.7$). Curve 4: the gas adsorption on a heterogeneous surface (θ_∞ =1, $K = 0.01$).

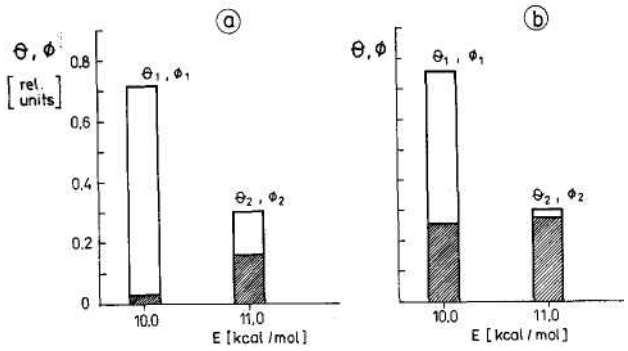

Fig. 2. Schematic diagrams of the discrete-energy spectra of the defect sites $\phi(E)$ and the degree of occupation of the defect sites by inert gas introduced at: (a) labelling pressure $\rho = 0.5$ relative units; and (b) labelling pressure $\rho = 10$ relative units. The effective activation energies E and corresponding degrees of occupation of the defect sites used are: $E_1 = 10$ kcal mol^{-1}, $\phi_1 = 0.7$, and $E_2 = 11$ kcal mo l^{-1}, $\phi_2 = 0.3$.

The schemes of the discrete-energy spectra $\phi(E)$ of the defect site and of the spectra of their occupation $\theta(E)$ under different inert gas pressure considered in this paper are demonstrated in Fig. 2.

From Fig. 2 it is obvious that the functions $\phi(E)$ and $\theta(E)$ for a single solid sample may differ substantially. Figure 2 illustrates schematically two discrete-energy spectra characterized by the energies E_1 and E_2 ($E_1 < E_2$) and the degrees of occupation ϕ_1 and ϕ_2 ($\phi_1 > \phi_2$). At low pressure the relative occupation (θ_1 and θ_2) of the energy sites E_1 and E_2 is $\theta_1 < \theta_2$, at medium pressures $\theta_1 \cong \theta_2$ and only at sufficiently high pressures does θ_1 become higher than θ_2. In practice this means that as the inert-gas pressure is increased, the defect sites of potential energy E_2 are occupied first. The redistribution of the inert-gas atoms between the potential-energy sites E_1 and E_2 depends on the temperature dependence of the equilibrium constant K. The defect sites of potential energy E_1 usually (at the low pressures used for sample labelling) contain a much lower amount of inert gas than do the defects of potential energy E_2. After the complete occupation of the defect sites of energy E_2, the occupation of the defect sites of energy E_1 takes place.

It is obvious that the inert-gas spectrum $\theta(E)$ reflected by the TGR curves may differ substantially as the partial pressure of the inert gas is changed. If this fact is neglected, substantial errors can be made in the interpretation of the TGR curves.

INFLUENCE OF THE INERT GAS PARTIAL PRESSURE ON THE TGR CURVES

The model solid sample contains defect sites of two types characterized by the energies E_1 and E_2 with degrees of occupation of ϕ_1 and ϕ_2, respectively, surrounded by the inert gas. The partial pressure of the inert gas is increased step-wise. The equation for the inert gas desorption kinetics can be written as

$$J = \sum_{1}^{k} \phi_i J_i \tag{5}$$

where k is the number of defect types in the energy spectrum, $J(T)$ is the inert gas flow from the sample (i.e. the TGR curve parameter), and J_i is the inert gas flow from the defect sites of the ith type, ϕ_i is the part of the ith type defects occupied by the inert gas.

Then, under isothermal conditions

$$J_i = -\frac{\mathrm{d}\theta}{\mathrm{d}T} = k_0 \exp\left(-\frac{E}{RT}\right)\theta \tag{6}$$

and under conditions of linearly rising temperature

$$J_i = \theta_0 k_0 \exp\left(-\frac{E}{RT}\right)\exp(\tau_i) \tag{7}$$

where

$$\tau_i = \frac{Ek_0}{R\beta}\left[\frac{-\exp(\xi)}{\xi} + Ei(\xi)\right]$$

where Ei is the integral exponential function and β is the heating rate. $Ei = \int_{-\infty}^{\xi} [\exp(t)/t]dt$ where ξ changes from $E/R(T_0 + \beta t)$ to E/RT_0.

Figure 3 shows the TGR curves computed for linearly rising temperature in the cases of the discrete defect-site spectra shown in Fig. 2. At low partial pressures the one-peak TGR curves result, as expected, in the energy of the defect sites determining the peak maximum J_{max}.

When the partial pressure of the inert gas during labelling is increased, the height of the $(J_{max})_2$ peak rises, in correspondence with the Langmuir isothermal curve. In Fig. 3, curve 3, it is shown that at a relative partial pressure of $\rho = 100$ during sample labelling, the maximum height of $(J_{max})_2$ is attained whereas the height of $(J_{max})_1$ increases.

At the high pressures of the inert gas used, $(T_{max})_1$ becomes most significant in the TGR curve. The importance of the sample labelling conditions on the TGR model curves has been shown here. The results have been used for the assessment of the functions $\theta(E)$ and $\phi(E)$ from the experimental TGR curves. The method of functional scales was used for the analysis of the TGR curves shown in Fig. 3. The results of this analysis are given in Fig. 4 as linear plots in the functional scale U versus $1/T$, assuming the energy distribution of the solid defects given in Fig. 2. It is obvious from Fig. 4 that at the low inert-gas pressure used for the sample labelling the slopes of the straight lines correspond to the energy value E_2. For the increased inert-gas pressure deviations from the straight lines were observed and the curves in the functional scale (see Fig. 4, curves 3 and 4) become S-like. At high inert-gas pressures the slopes of the linear parts of this relationship correspond to the E_1 value.

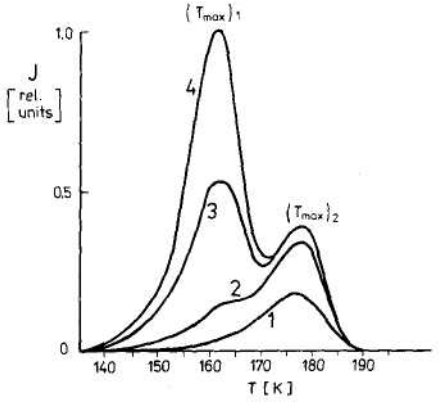

Fig. 3. The model curves of the thermostimulated inert gas release (TGR curves) computed for the case of the defect sites of two discrete energy lines (E_1 =10 kcal mol^{-1} $\phi_1 = 0.7$, $K = 0.01$; and E_2=11 kcal mol^{-1}, $\phi_2 = 0.3$, $K = 1$) and different partial pressures during sample labelling. The pre-exponential factor .K_0 =10^{13} s^{-1} and the linear heating rate β = 2 K s^{-1} were supposed. Curves 1 - 4 correspond to relative partial pressures of (in relative units): 1, 10, 100 and saturation gas pressure, respectively.

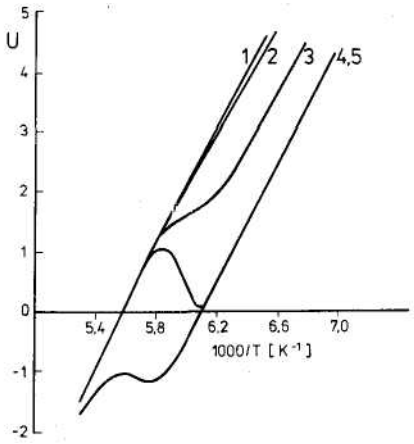

Fig. 4. Influence of the partial pressure of the gas used during sample labelling on the TGR curves represented in the functional scales. The kinetics of the single-jump diffusion (first-order chemical reaction) were assumed. Curves 1-5 correspond to the partial pressures *(p,* in relative units): ρ = 0.05, 1.01, 10.0, 100 and the saturation gas pressure, respectively.

An alternative method is based on the analysis of the temperature dependence of the effective activation energy E_{ef}. The plots of E_{ei} versus temperature for the inert-gas partial pressures used for sample labelling are shown in Fig. 5. This method was used to evaluate the TGR curves given in Fig. 3. The samples studied were characterized by their discrete-energy spectra, as shown in Fig. 2. Curves 1-4 in Fig. 5 describe the conditions of the sample labelling varying by two-orders of magnitude.

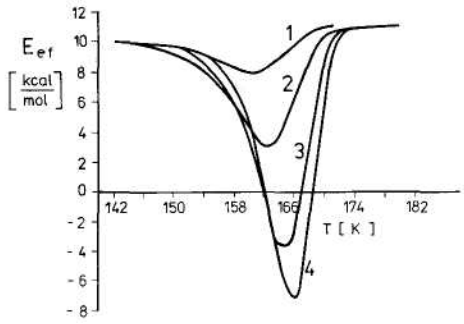

Fig. 5. The temperature dependences of the effective activation energy of thermostimulated gas release (TGR curves). Curves 1-4 correspond to the partial pressures (in relative units): 1, 10, 100 and saturation gas pressure, respectively.

The energy value E_1 = 10 kcal mol^{-1} was determined from the initial parts of all the curves in Fig. 5 (i.e. for all values of the partial pressure used), whereas the energy value E_2 = 11 kcal mol^{-1} was determined from the terminal part of the curves (i.e. under the conditions of high pressure).

THE INFLUENCE OF PRELIMINARY SAMPLE OUTGASSING ON THE TGR CURVES

In addition to the factors described above the amount of inert gas located at the defect sites of solids also depends on the preliminary thermal treatment of the solid samples. Here we analyse the solid sample characterized by the discrete-energy spectrum shown in Fig. 2, obtained by the diffusion technique of labelling at partial pressures which ensured the complete occupation of the defect sites by the inert gas. The preliminary thermal treatment caused the partial outgassing of the labelled sample.

The choice of a suitable temperature and duration of the thermal treatment makes it possible to influence the shape of the TGR curves. Therefore, the determination of the energy spectrum of the inert gas labelling, $\theta(E)$, can be simplified. Let us suppose that the preliminary thermal treatment occurs at the constant temperature T and a time period t. The concentration of the inert gas located at the defect sites of the z'th type decreases with time as

$$\theta(t) = \theta_0 \exp(-kt) \tag{8}$$

where k is the diffusion rate constant, $k = k_0 \exp(- E/RT_0)$. During thermal treatment at temperature T_o of duration t, the concentration of the inert gas label is expressed by

$$\theta(t) = \theta_0 \exp\left[-\exp\left(-\frac{E}{RT} + \tau\right)\right] \tag{9}$$

where $\tau = \ln(tk_0)$.

Figure 6 shows the model TGR curves computed for the samples whose energy spectra are given in Fig. 2, and for preliminary sample outgassing at 140 K assuming various time intervals for the sample outgassing. It can be seen from Fig. 6 that the height of the first peak diminished with increasing duration of the thermal treatment. When the treatment is sufficiently long, the first peak disappears completely and the second peak diminishes substantially.

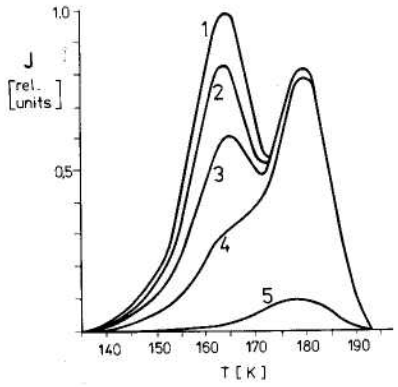

Fig. 6. Model curves of the thermostimulated gas release computed for the linear heating rate $\beta = 2$ K s^{-1} and the partial outgassing of samples at 140 K. The defect sites characterized in Fig. 2 were assumed. Curves 1-5 correspond to preliminary outgassing durations of: 0, 5, 6, 7 and 11 relative units, respectively.

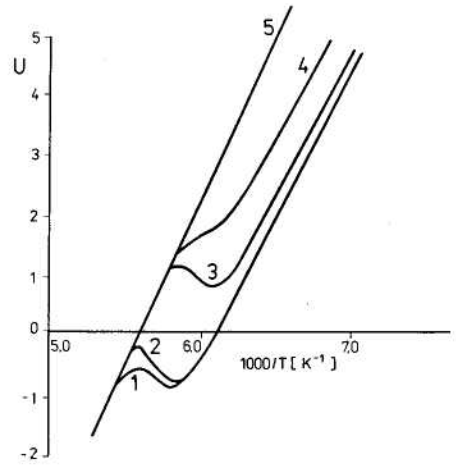

Fig. 7. The influence of sample outgassing on the TGR curves represented in the functional scale. The kinetics of the single-jump diffusion were assumed. Curves 1-5 correspond to various durations of sample outgassing at 140 K: 0, 5, 6, 7 and 11 relative time units, respectively.

It was demonstrated that the energy values E_1 and E_2 can be easily determined from the slopes of the linear parts of the functional-scale plots when the labelled samples are outgassed at a suitable temperature and for a suitable time. Figure 7 shows the computed curves in the functional scales U versus $1/T$ corresponding to the model TGR curves given in Fig. 6. The values E_1 and E_2 were determined in the same way as described for Fig. 4.

CONCLUSION

It has been shown that the shape of TGR curves depends substantially on the labelling conditions of the samples. The shape of the TGR curves suitable for the assessment of the energy spectrum of the solid-state defects can be obtained by varying the inert-gas pressure during sample labelling and the time duration of the labelling process. The results obtained can be used in interpreting ETA experimental results.

REFERENCES

1 A.V. Zheleznov, I.N. Beckman and V. Balek, Thermochim. Acta, 142 (1989) 251.
2 A.A. Shviryaev, I.N. Beckman and V. Balek, Thermochim. Acta, 111 (1987) 215.
3 R.B. McLellan, Acta Metal., 27 (1979) 1655.